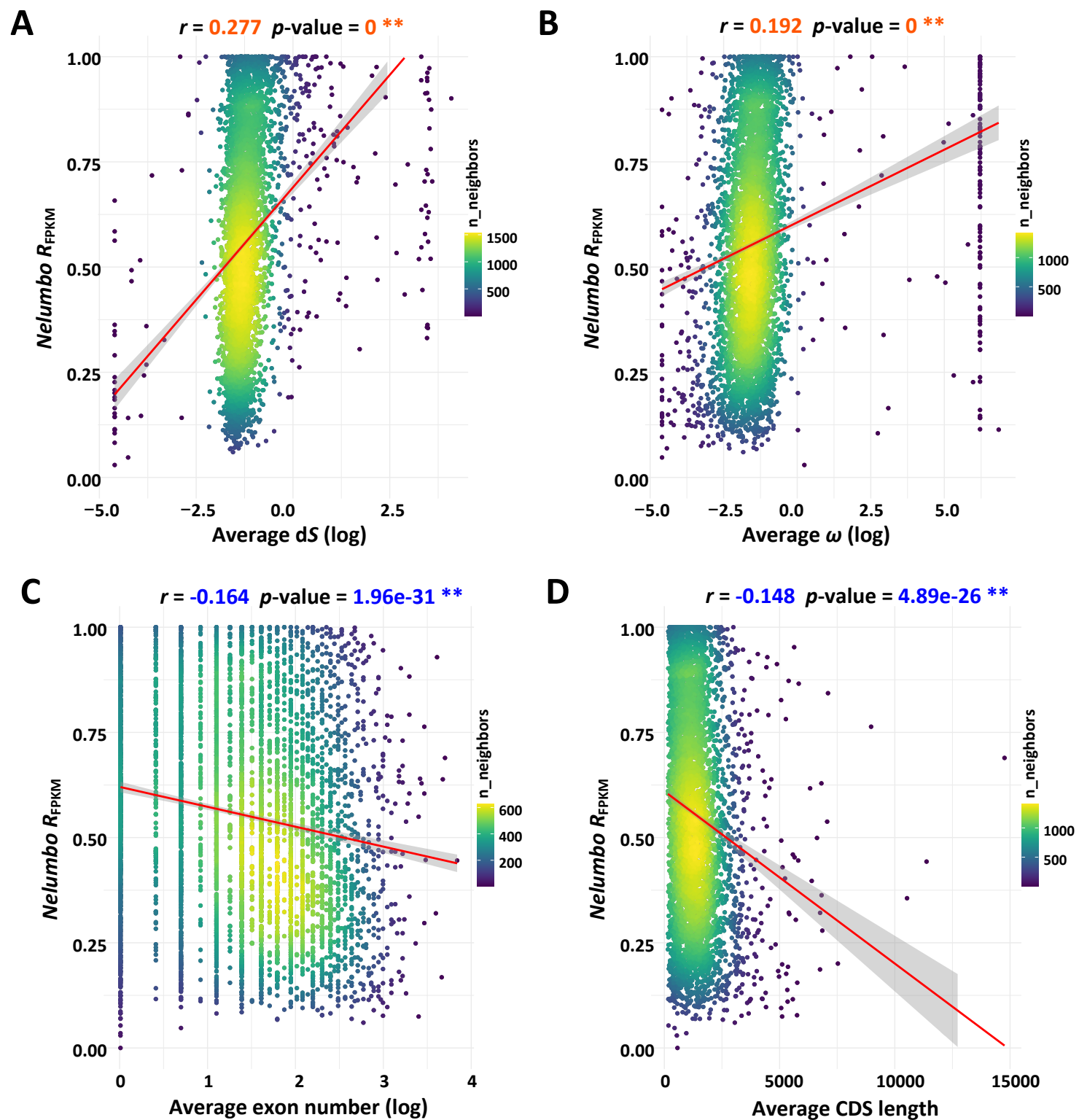
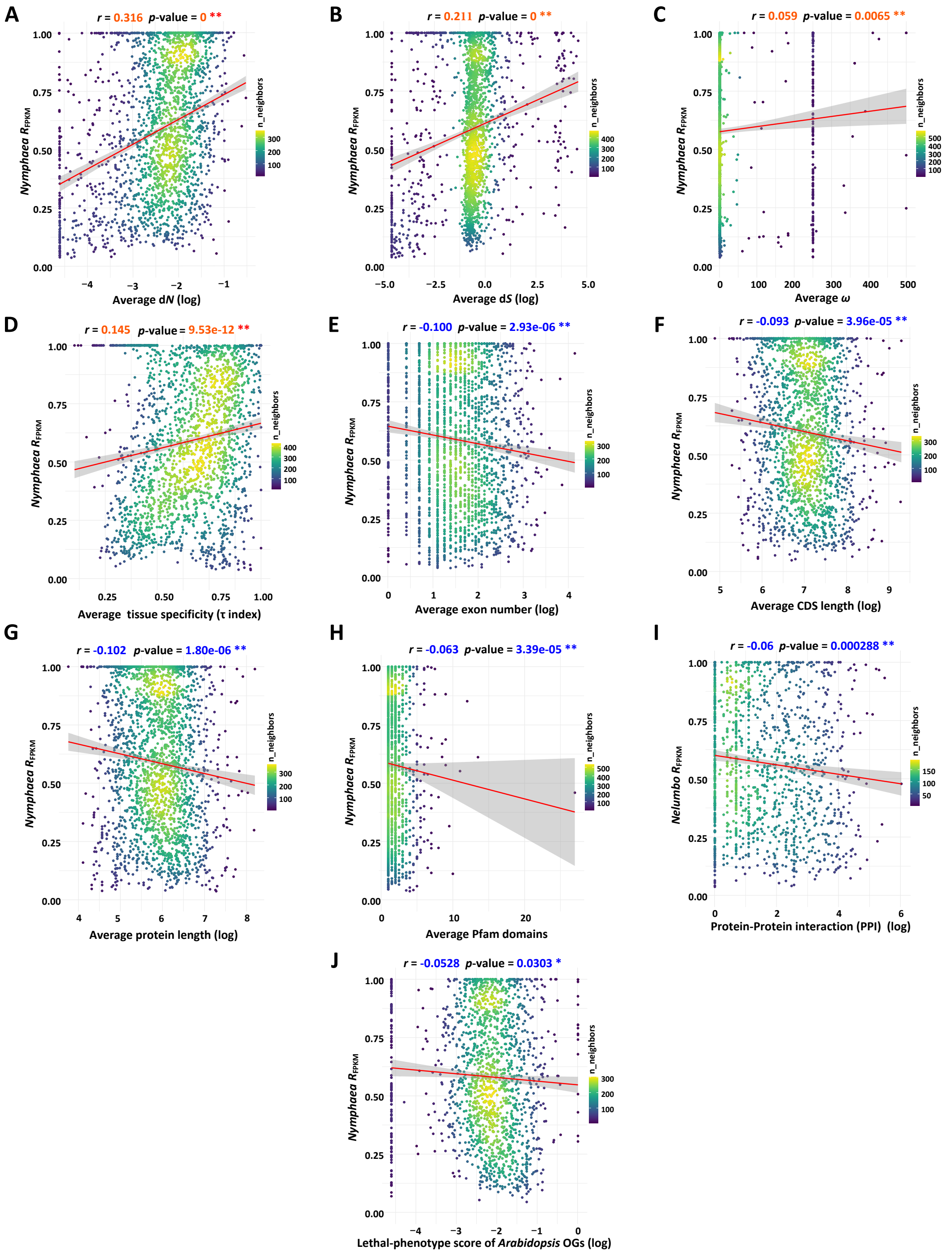


**Supplementary Figure S1. Pearson correlations of relative expression differences ( $R_{\text{FPKM}}$ ) of WGD duplicates between different tissues. **A.** Between leaf and petiole in *Nelumbo*. **B.** Between juvenile leaf and juvenile leafstalk in *Nymphaea*. **C.** Between young leaf and old leaf in *Acorus*. WGD, whole genome duplication; FPKM, fragments per kilobase of exon model per million mapped fragments; grey shading band, the 95% (default) confidence level interval for predictions from a linear model; red font, positive correlation; \*\*,  $p$ -value < 0.01.**

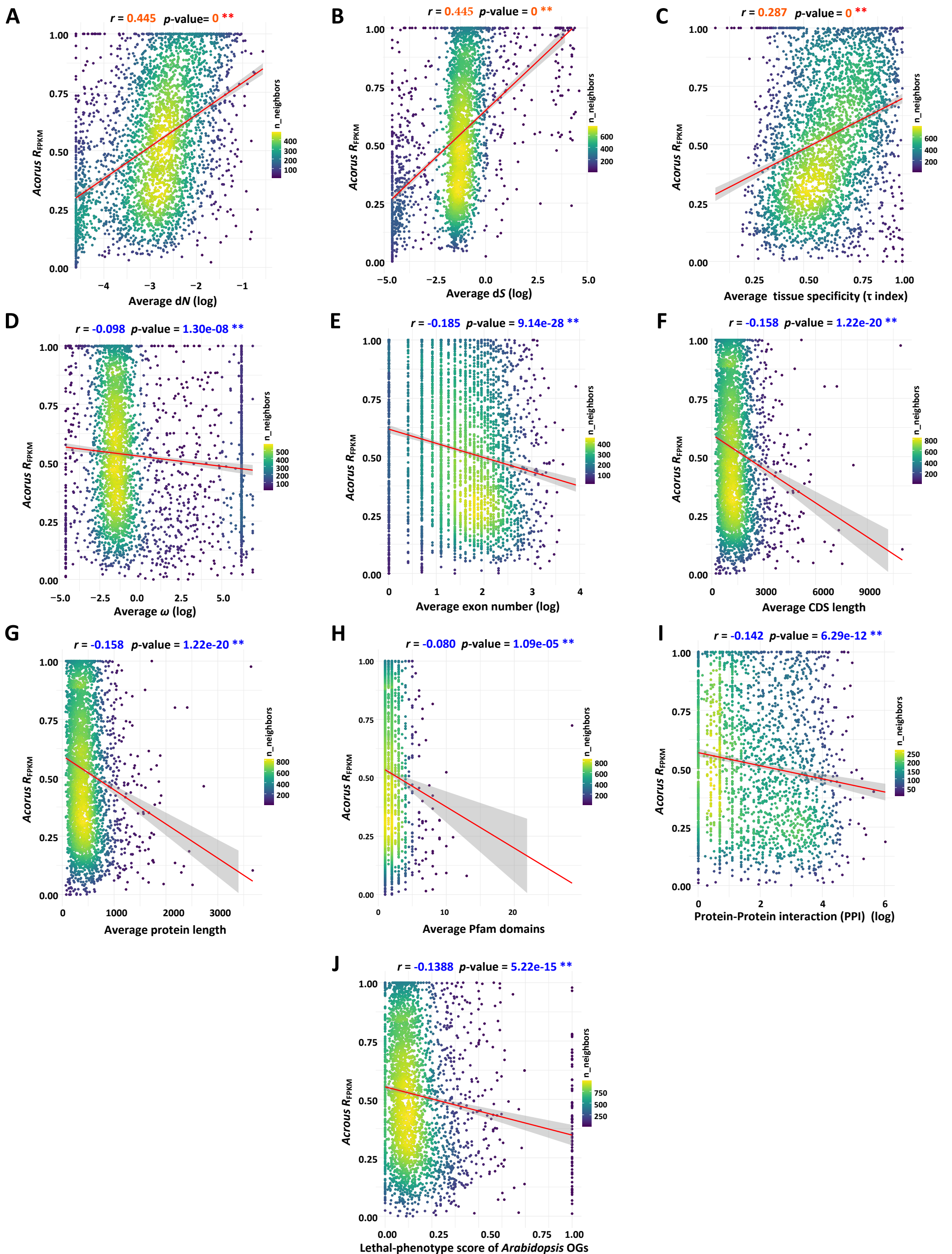


**Supplementary Figure S2. Pearson correlations between average relative expression differences ( $R_{\text{FPKM}}$ ) of WGD duplicates and gene features in *Nelumbo*.** **A-B.** Average  $R_{\text{FPKM}}$  of WGD duplicates are significantly positively correlated with average synonymous substitutions per site (dS) after WGD (**A**) and average  $\omega$  (dN/dS ratio) after WGD (**B**). **C-D.** Average  $R_{\text{FPKM}}$  of WGD duplicates are significantly negatively correlated with average exon number (**C**) and average coding sequence (CDS) length (**D**). WGD, whole genome duplication; FPKM, fragments per kilobase of exon model per million mapped fragments;  $r$ , correlation coefficient of Pearson correlation test; log, log-transformed values of gene features in x-axis; grey shading band, the 95% (default) confidence level interval for predictions from a linear model; red font, positive correlation; blue font, negative correlation; \*\*,  $p\text{-value} < 0.01$ .



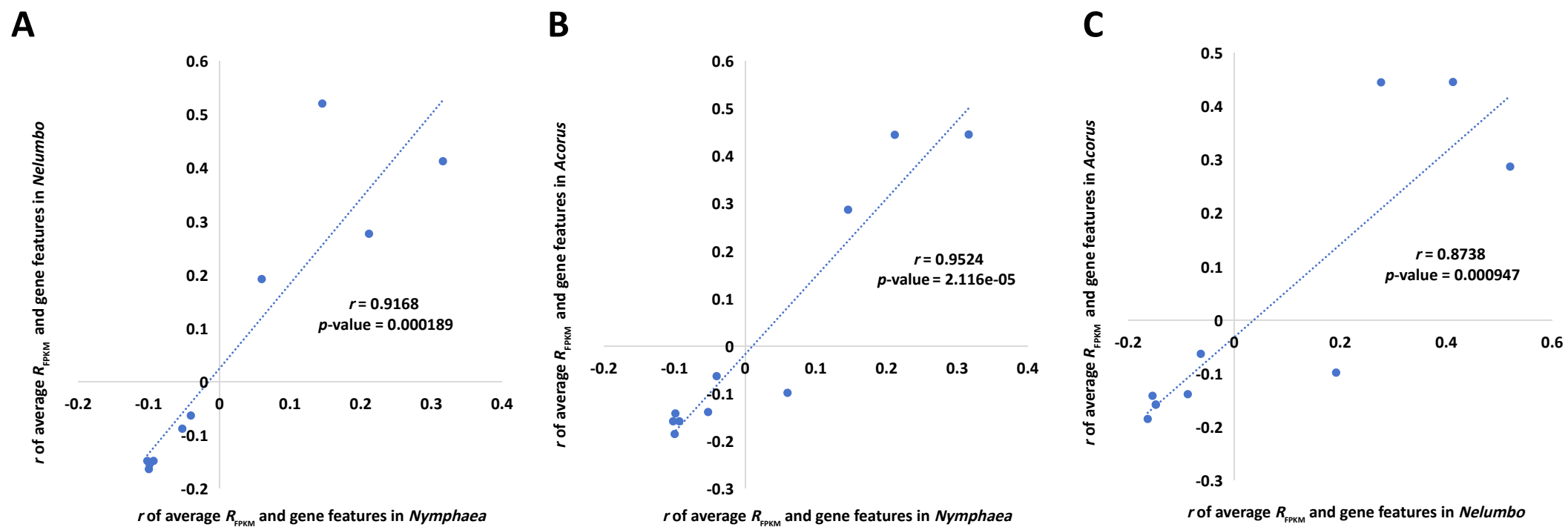


**Supplementary Figure S3. Pearson correlations between average relative expression differences ( $R_{\text{FPKM}}$ ) of WGD duplicates and gene features in *Nymphaea*. A-D.** Average  $R_{\text{FPKM}}$  of WGD duplicates are significantly positively correlated with average non-synonymous substitutions per site (dN) after WGD (A), average synonymous substitutions per site (dS) after WGD (B), average  $\omega$  (dN/dS ratio) after WGD (C), tissue specificity ( $\tau$ ) of gene expression (D). E-J. Average  $R_{\text{FPKM}}$  of WGD duplicates are significantly negatively correlated with average exon number (E), average coding sequence (CDS) length (F), average protein length (G), No. of Pfam domains genes (H), No. of protein-protein interactions (PPIs) of putative orthologs in *Arabidopsis* (I), lethal-phenotype score of *Arabidopsis* putative ortholog groups (J). WGD, whole genome duplication; FPKM, fragments per kilobase of exon model per million mapped fragments;  $r$ , correlation coefficient of Pearson correlation test; log, log-transformed values of gene features in x-axis; grey shading band, the 95% (default) confidence level interval for predictions from a linear model; red font, positive correlation; blue font, negative correlation; \*,  $p\text{-value} < 0.05$ ; \*\*,  $p\text{-value} < 0.01$ .

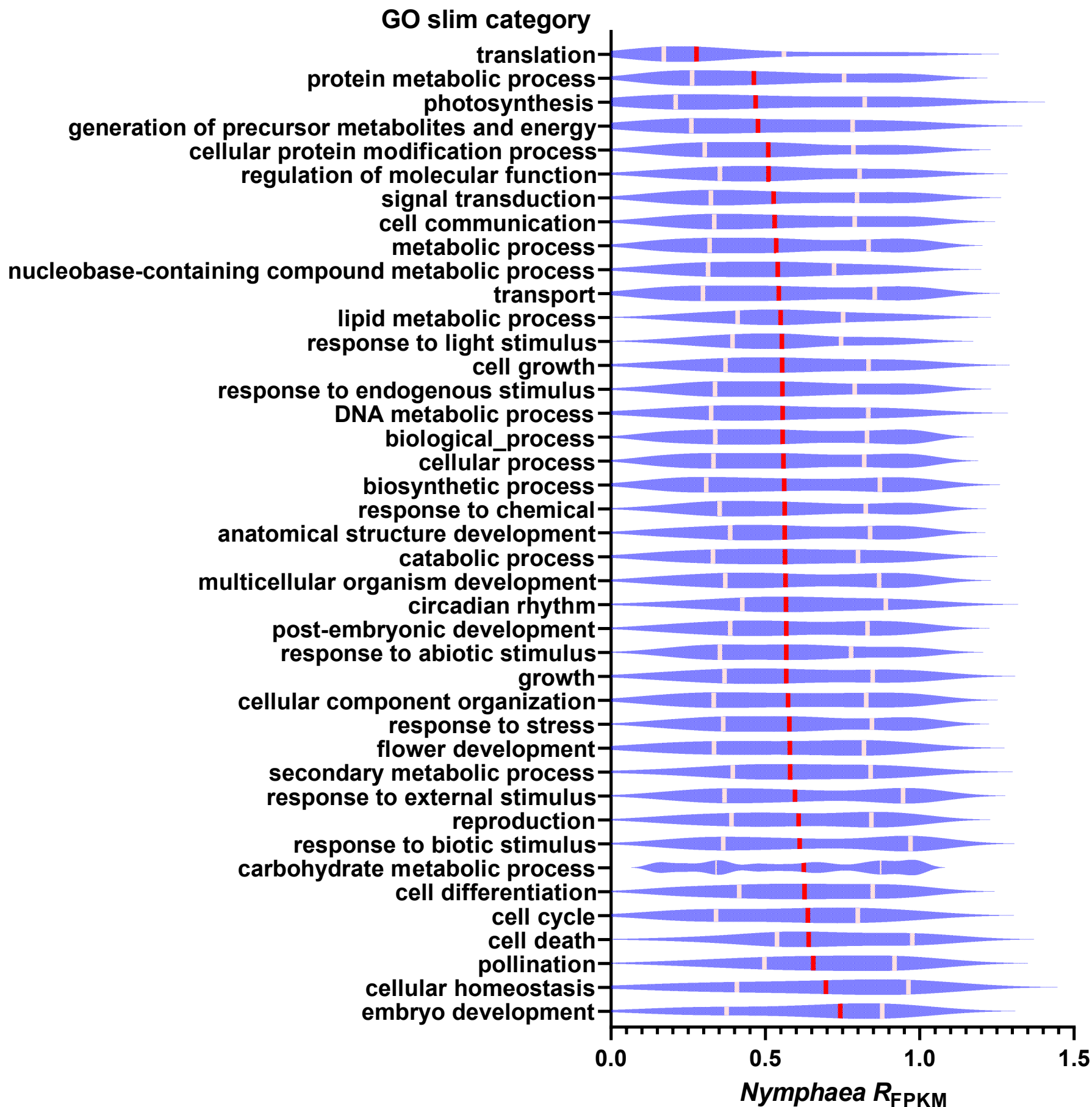


**Supplementary Figure S4. Pearson correlations between average relative expression differences ( $R_{\text{FPKM}}$ ) of WGD duplicates and gene features in *Acorus*.** **A-C.** Average  $R_{\text{FPKM}}$  of WGD duplicates are significantly positively correlated with average non-synonymous substitutions per site ( $dN$ ) after WGD (**A**), average synonymous substitutions per site ( $dS$ ) after WGD (**B**), and tissue specificity ( $\tau$ ) of gene expression (**C**). **D-J.** Average  $R_{\text{FPKM}}$  of WGD duplicates are significantly negatively correlated with average  $\omega$  ( $dN/dS$  ratio) after WGD (**D**), average exon number (**E**), average coding sequence (CDS) length (**F**), average protein length (**G**), No. of Pfam domains genes (**H**), No. of protein-protein interactions (PPIs) of putative orthologs in *Arabidopsis* (**I**), lethal-phenotype score of *Arabidopsis* putative ortholog groups (**J**). WGD, whole genome duplication; FPKM, fragments per kilobase of exon model per million mapped fragments;  $r$ , correlation coefficient of Pearson correlation test; log, log-transformed values of gene features in x-axis; grey shading band, the 95% (default) confidence level interval for predictions from a linear model; red font, positive correlation; blue font, negative correlation; \*,  $p\text{-value} < 0.05$ ; \*\*,  $p\text{-value} < 0.01$ .



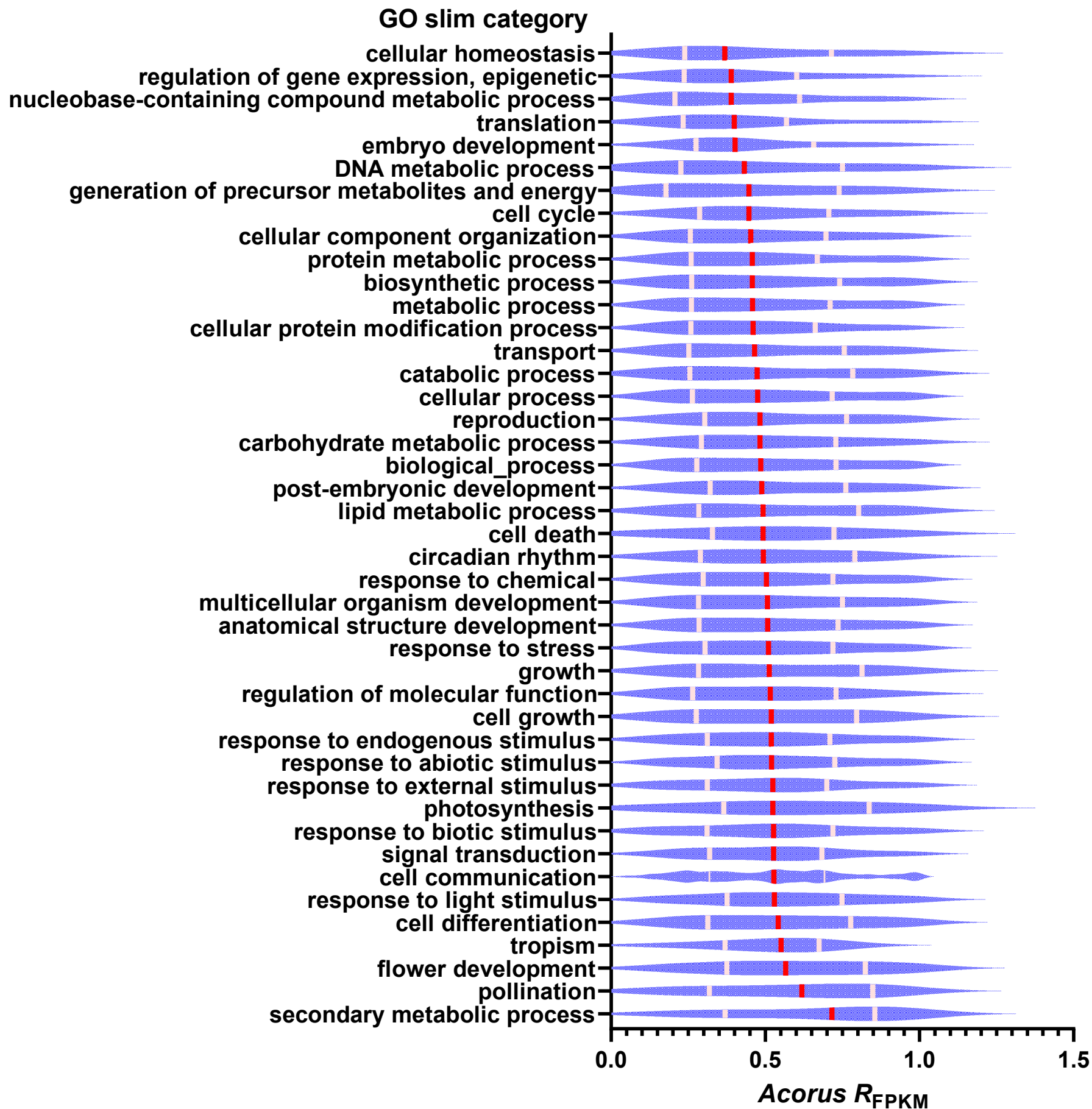


**Supplementary Figure S5. Pearson correlations of the correlation coefficients ( $r$ ) of average relative expression ( $R_{\text{FPKM}}$ ) and gene features among three species. (A)  $r$  of average  $R_{\text{FPKM}}$  and gene features between *Nymphaea* and *Nelumbo*. (B)  $r$  of average  $R_{\text{FPKM}}$  and gene features between *Nymphaea* and *Acorus*. (C)  $r$  of average  $R_{\text{FPKM}}$  and gene features between *Nelumbo* and *Acorus*. FPKM, fragments per kilobase of exon model per million mapped fragments. Gene features were listed in Supplementary Table S6.**

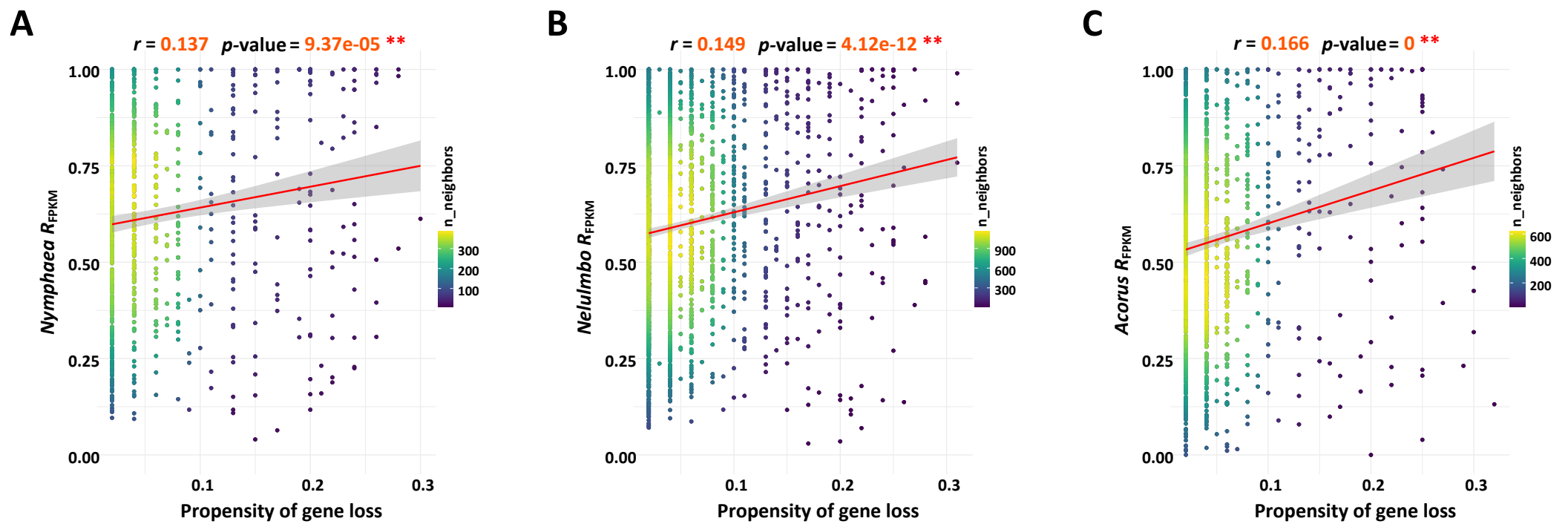


**Supplementary Figure S6. Violin plot showing how the relative expression difference ( $R_{\text{FPKM}}$ ) for *Nymphaea* homoeologs varies among duplicate genes belonging to different Gene Ontology (GO) slim categories. FPKM, fragments per kilobase of exon model per million mapped fragments; red bar, median; pink bar, quartile. The sample sizes of the GO slim categories, from bottom to top in the figure, are as follows: 37, 14, 17, 14, 28, 81, 44, 103, 125, 139, 25, 32, 244, 172, 47, 206, 126, 13, 212, 85, 243, 268, 183, 660, 955, 19, 180, 40, 80, 41, 181, 78, 485, 153, 122, 35, 131, 42, 32, 213 and 48.**

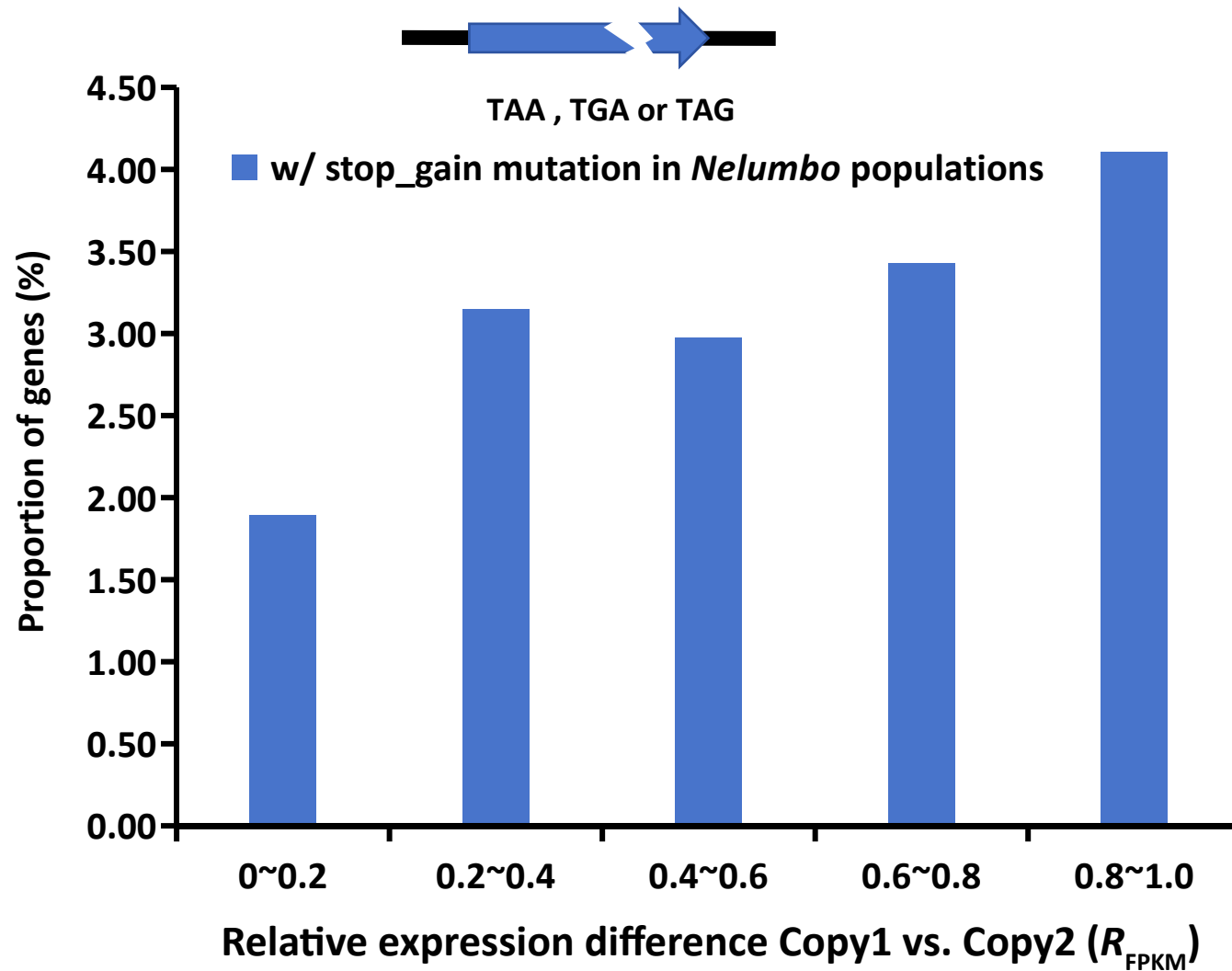




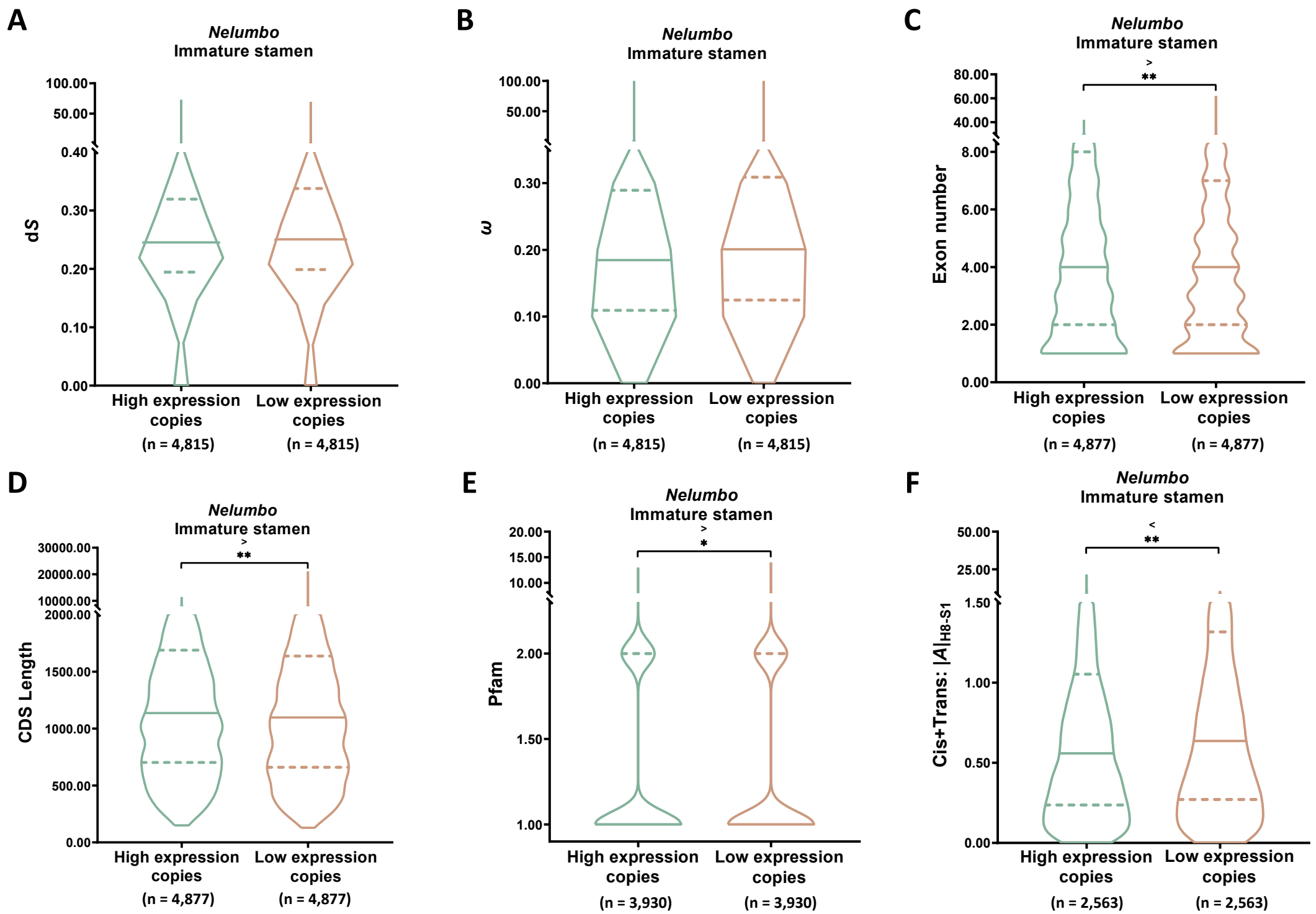
**Supplementary Figure S7. Violin plot showing how the relative expression difference ( $R_{\text{FPKM}}$ ) of *Acorus* homoeologs varies among duplicate genes belonging to different Gene Ontology (GO) slim categories.** FPKM, fragments per kilobase of exon model per million mapped fragments; red bar, median; pink bar, quartile. The sample sizes of the GO slim categories, from bottom to top in the figure, are as follows: 43, 30, 62, 16, 149, 106, 219, 192, 165, 16, 222, 353, 281, 54, 67, 66, 445, 426, 365, 463, 21, 17, 109, 222, 1559, 72, 218, 1110, 164, 248, 247, 847, 302, 360, 302, 52, 34, 39, 68, 50, 194, 24 and 21.



**Supplementary Figure S8. Pearson correlations between average relative expression differences ( $R_{\text{FPKM}}$ ) of WGD duplicates and propensity of gene loss. A. *Nymphaea*. B. *Nelumbo*. C. *Acorus*. WGD, whole genome duplication; FPKM, fragments per kilobase of exon model per million mapped fragments; grey shading band, the 95% (default) confidence level interval for predictions from a linear model; red font, positive correlation; \*\*,  $p$ -value < 0.01.**

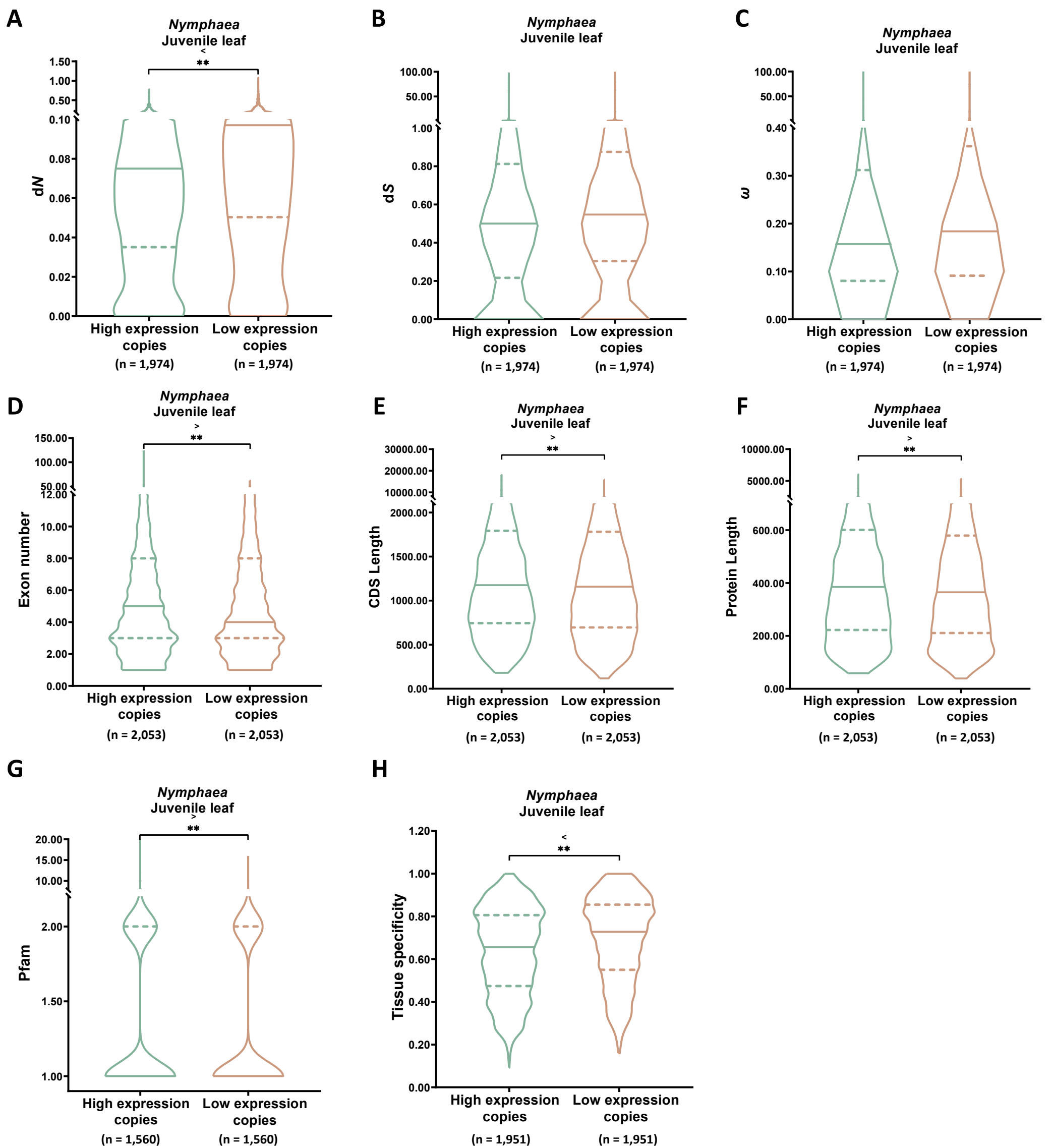


**Supplementary Figure S9. Distributions of the proportion of genes with premature stop codon mutations in *Nelumbo* populations according to relative expression difference between the two copies ( $R_{\text{FPKM}}$ ).** FPKM, fragments per kilobase of exon model per million mapped fragments.



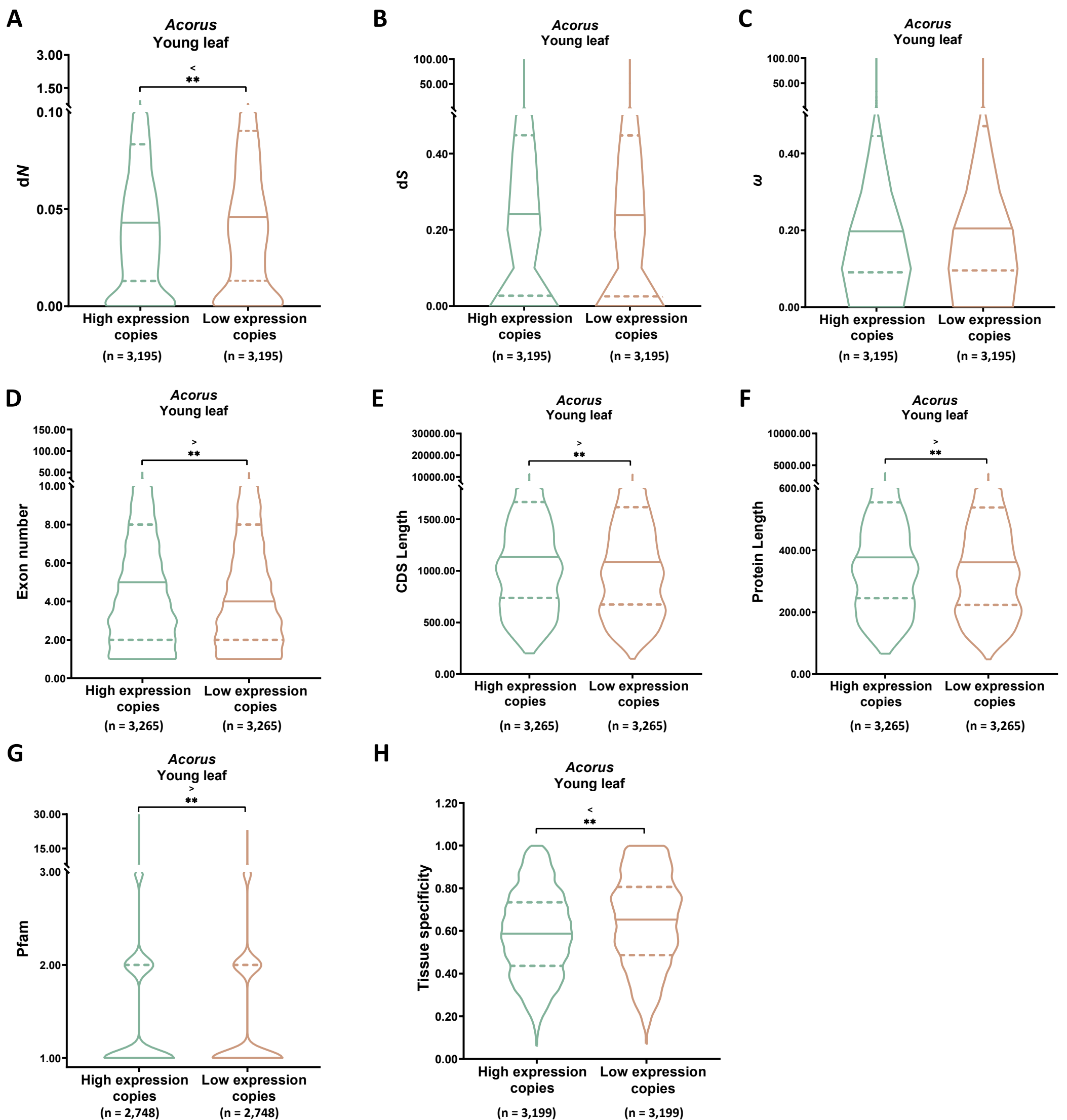
**Supplementary Figure S10. Differences between homoeologs with higher and lower gene expression in immature stamen of *Nelumbo*.** Differences in synonymous substitutions per site (dS) after whole-genome duplication (WGD) (**A**),  $\omega$  (dN/dS ratio) after WGD (**B**), exon number (**C**), coding sequence (CDS) length (**D**), No. of Pfam domains of genes (**E**), *cis*- and *trans*-regulatory change magnitude (H8-S1) (**F**) between homoeologs with higher expression and lower expression in immature stamen of *Nelumbo* (paired *t* tests, \*\* *p*-value < 0.01, \* *p*-value < 0.05). Solid line in violin plot, median value; dashed line in violin plot, quantile; n, sample size.



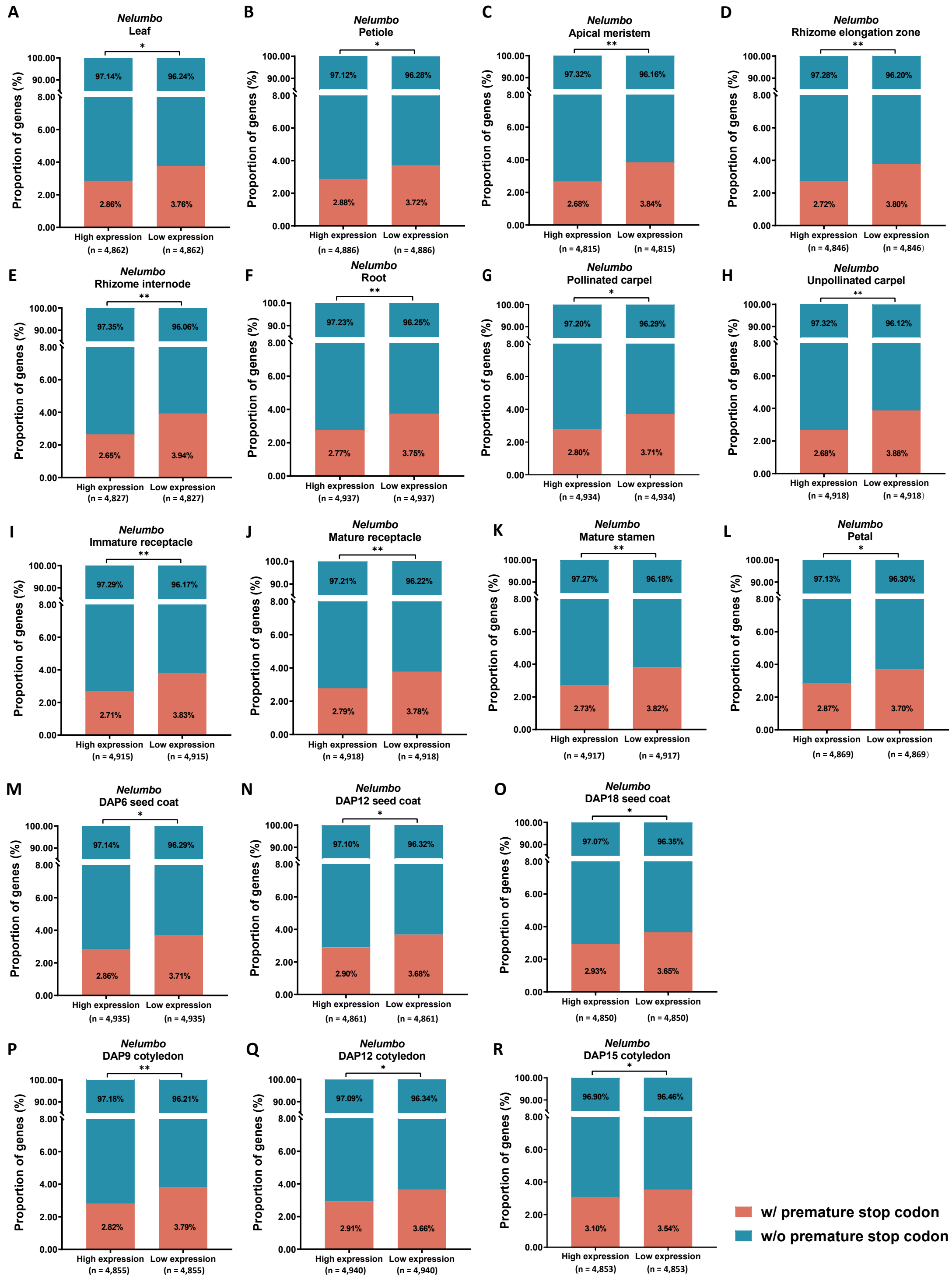


**Supplementary Figure S11. Differences between homoeologs with higher and lower gene expression in juvenile leaf of *Nymphaea*.**

Differences in non-synonymous substitutions per site (dN) after whole-genome duplication (WGD) (**A**), synonymous substitutions per site (dS) after WGD (**B**),  $\omega$  (dN/dS ratio) after WGD (**C**), exon number (**D**), coding sequence (CDS) length (**E**), protein length (**F**), No. of Pfam domains of genes (**G**), tissue specificity ( $\tau$  index) of gene expression (**H**) between homoeologs with higher expression and lower expression in juvenile leaf of *Nymphaea* (paired *t* tests, \*\* *p*-value < 0.01). Solid line in violin plot, median value; dashed line in violin plot, quantile; n, sample size.



**Supplementary Figure S12. Differences between homoeologs with higher and lower gene expression in young leaf of *Acorus*.** Differences in non-synonymous substitutions per site (dN) after whole-genome duplication (WGD) (**A**), synonymous substitutions per site (dS) after WGD (**B**),  $\omega$  (dN/dS ratio) after WGD (**C**), exon number (**D**), coding sequence (CDS) length (**E**), protein length (**F**), No. of Pfam domains of genes (**G**), tissue specificity ( $\tau$  index) of gene expression (**H**) between homoeologs with higher expression and lower expression in young leaf of *Acorus* (paired *t* tests, \*\* *p*-value < 0.01). Solid line in violin plot, median value; dashed line in violin plot, quantile; n, sample size.



**Supplementary Figure S13. Differences in premature stop codon mutations in *Nelumbo* populations between homoeologs with higher expression and lower expression in 19 different tissues of *Nelumbo*.  $\chi^2$  test, \*\*  $p$ -value < 0.01, \*  $p$ -value < 0.05; n, sample size.**